Research Article

Valentina Biagioni
Claudia Venditti
Alessandra Adrover*
Stefano Cerbelli

Fractionation of a Three-Particle Mixture by Brownian Sieving Hydrodynamic Chromatography

Particles ranging in size from a few nanometers (exosomes or viruses) to a few micrometers (bacteria or red blood cells) can be sorted using a size-based separation process. One of the simplest techniques is provided by hydrodynamic chromatography (HDC) which typically requires long channels to achieve adequate resolution. A new separation mechanism based on a Brownian sieving effect coupled with HDC has recently been proposed to overcome these limitations. An efficiency improvement of up to 2000 % has been predicted for a two-size mixture. The aim of this work is to study and optimize a modified geometry useful for obtaining the simultaneous separation of a three-size diluted suspension. The results suggest a significant performance improvement, up to 3000 %, over the standard HDC.

1 Introduction

The size-based fractionation of multi-dispersed suspensions of micrometric/nanometric characteristic size constitutes a fundamental operation in many contexts, ranging from analytical operations to small/intermediate-scale productions of high-added-value products, e.g., gold nanoparticles used in cancer therapy [1], and vectors for DNA- and RNA-based vaccines [2]. For this reason, novel separation techniques, such as field-flow fractionation (FFF) [3, 4], hydrodynamic chromatography (HDC) [5–9], and deterministic lateral displacement (DLD) [10–13], have been proposed.

Among these techniques, HDC is attracting increasing interest in view of its flexibility and simplicity. The core of the HDC device is a plain empty microcapillary. The separation principle is based on the interaction between a non-uniform axial velocity profile attained by the eluent in the presence of a pressure drop within the channel, and the existence of transversal Brownian motion of the latter due to thermal fluctuations. Because the center of mass of large particles cannot reach the solid surfaces delimiting the flow, under the traversal diffusive motion they can only jump between high-velocity streamlines. By this mechanism, the average particle velocity within the channel is an increasing function of the particle size, making it possible to perform a size-based separation under transient conditions.

HDC is commonly applied for the characterization of polymer mixtures, however, it requires lengthy channels to obtain an adequate resolution between particles of different size. Recently, a new device with a two-coaxial channel geometry has been designed [14–16], where the HDC separation drive is combined with a Brownian sieving (BS) mechanism to boost the efficiency of the separation between particles below and above a critical size. Enhancement factors of order 20 with respect to the standard HDC device have been predicted, meaning that the BS-HDC column length is 2000 % shorter than the HDC capillary [14] with the same resolution (separation efficiency).

In this work, a double Brownian sieving (DBS) mechanism in a three-coaxial channel geometry is investigated (see Fig. 1) with the aim to simultaneously sort a suspension of particles of three different diameters, namely, $d_1 > d_2 > d_3$.[1] The internal and the intermediate channels communicate through fixed openings with width equal to λ_1, where $d_2 < \lambda_1 < d_1$, i.e., smaller than larger particles and larger than medium-sized and smaller particles. The external and the intermediate annular channels communicate by openings with size equal to $\lambda_2 < \lambda_1$, where $d_3 < \lambda_2 < d_2$, i.e., smaller than large and medium-sized particles and larger than smaller particles. The three-dimensional channel is created by alternately extruding the cross-sectional pro-

---

Dr. Valentina Biagioni, Dr. Claudia Venditti, Prof. Alessandra Adrover
https://orcid.org/0000-0001-5939-740X,
Prof. Stefano Cerbelli https://orcid.org/0000-0003-3906-6595
(alessandra.adrover@uniroma1.it)
Dipartimento di Ingegneria Chimica Materiali Ambiente, Sapienza Università di Roma, Via Eudossiana 18, 00184 Roma, Italy.
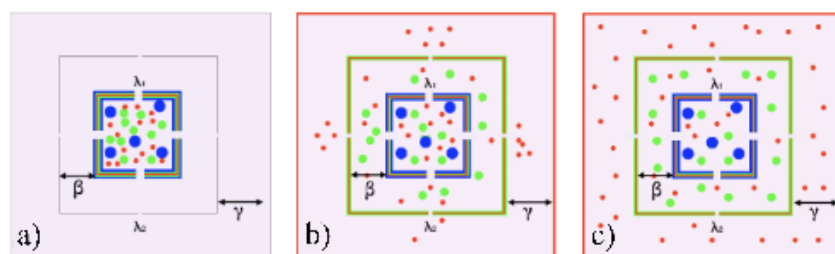
 Wiley Online Library
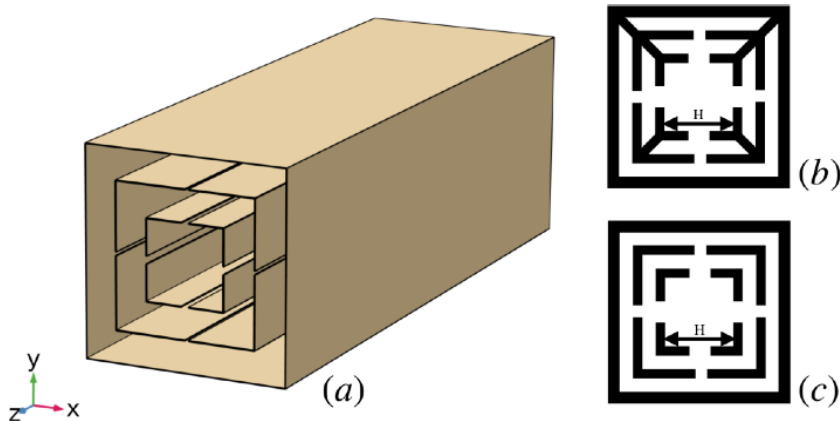
Figure 1. (a) Three-channel geometry of the double Brownian sieving device (DBS-HDC); (b, c) cross-sectional masks.

files in Figs. 1b, c so that the internal channels can be held in place by the bearings slanted at 45°. The manufacturing of the device is ideally suited for 3D-nanoprinting.

The suspension is initially loaded inside the internal channel, and a pressure-driven flow is started, which drags the particles downstream the device. As the particles flow through the device, smaller particles can access the second and the third channel by transverse diffusion, therefore reaching a uniform distribution throughout the entire three-channel cross section. Medium-sized particles can access only the second channel, by the same mechanism. Conversely, larger particles are trapped in the core channel, as shown in Fig. 2.

In the two-channel geometry, the thickness of the annular channel has been chosen to maximize the difference in average velocity of the eluent between the two channels. In this case, the geometry, controlled by the thicknesses of the intermediate (β) and external (γ) annular channels, is chosen to maximize the difference between the average velocity pertaining to each channel. The optimization of the device can be accomplished by extending the approach developed in [15], based on Brenner's macro transport theory, to the modified geometry. Results suggest that for the three-size suspension the DBS mechanism enhancement is up 3000 % with respect to the same three-size separation in the classical HDC channel.

2 Theoretical Setting

This section focuses on the transport model used to quantify the separation performance of the DBS hydrodynamic chromatography microcapillary (henceforth DBS-HDC). An infinitely long microcapillary with axial coordinate z and cross section $\Omega(x,y)$ is considered. By enforcing the one-way-coupling approximation, the velocity field of the suspending fluid can be computed independently from the particle dynamics. Due to the micrometric size of the cross section, the Reynolds number is well below unity, so that the laminar flow regime is prevailing, and the velocity field only consists of the axial component $w(x,y)$, which only depends on the x and y cross-sectional coordinates. The velocity profile can therefore be evaluated by solving a single 2D Poisson equation with respect to $w(x,y)$:

$$\nabla_\perp^2 w = \frac{1}{\mu}\frac{\partial p}{\partial z}, \quad \nabla_\perp^2 = \frac{\partial^2}{\partial x^2} + \frac{\partial^2}{\partial y^2} \tag{1}$$

endowed with no-slip boundary conditions $w = 0$ on the boundary $\partial\Omega$ which consists of the physical walls of the cross section and the internal baffles. In Eq. (1), μ is the dynamic viscosity, $\nabla_\perp^2$ is the cross-sectional Laplacian operator, and p is the hydrodynamic pressure. Whilst the solution of Eq. (1) can be obtained at relatively low computational cost, a direct approach to the dynamics of the suspended particles poses severe computational issues. Specifically, the evolution of the particle distribution, defined by the particle number density $n(x,y,z,t)$, is governed by a 3D transient advection-diffusion equation:

$$\frac{\partial n}{\partial t} + w(x,y)\frac{\partial n}{\partial z} = D_P\left(\nabla_\perp^2 n + \frac{\partial^2 n}{\partial z^2}\right), \quad D_P = \frac{k_b T}{6\pi\mu r_P} \tag{2}$$

equipped with Neumann boundary conditions (impermeability conditions) on the solid-fluid interfaces. In Eq. (2), D_P is the particle diffusivity which, for a supposedly spherical particle, can be derived from the Stokes-Einstein relationship. The multiscale nature of this equation makes its numerical solution unfeasible, in that it requires an exceedingly large number of degrees of freedom because both the cross-sectional lengthscale and the ever-growing axial lengthscale characterizing the particle distribution need be resolved; in practical application the latter can be 100–10 000 times the first.

Particles are subjected to isotropic Brownian diffusion and to the suspending flow, meaning that it is assumed that their center of mass tracks the flow streamlines (overdamped regime). This is valid for particles supposedly massless as well as fort particles characterized by a finite size. The finite size can be easily considered by adopting an excluded-volume approach. Because the

Figure 2. Cross section of the DBS-HDC. Blue, green, and red circles represent respectively the big, medium, and small particles with diameters $d_3 < \lambda_2 < d_2 < \lambda_1 < d_1$. The excluded volume is depicted with the same color as the corresponding particle size. (a) Inlet condition; (b) particle spreading at short-intermediate timescales; (c) longer timescales.

size of the particle is non-vanishing, there exists a minimal distance between the particle center of mass and the walls confining the channel, so that streamlines that pass near the walls closer than this distance cannot be sampled by the particles. This region is referred to as excluded volume and increases with the particle size.

Since at increasing particle diameters, larger and larger portions of the low-velocity near-wall region are excluded from the average, the portion of the cross section Ω_p accessible to the particle decreases with the particle radius d_p and the average particle velocity rises with particle size (see Fig. 2). The reliability of the excluded volume approach has been checked with experimental data in complex geometries, as reported in [13], and through the comparison with results obtained with a more accurate and detailed two-way coupling approach [16].

In the light of this, the fundamental result of Brenner macrotransport theory [17] is the possibility to reduce the evolution of the particle number density, $n(x,y,z,t)$ to an effective transport equation involving a cross-averaged concentration $C(z,t)$, which at large time scales reads as:

$$\frac{\partial C}{\partial t} + W_p^{\text{eff}} \frac{\partial C}{\partial z} = D_p^{\text{eff}} \left(\frac{\partial^2 C}{\partial z^2} \right) \tag{3}$$

The effective transport parameter W_p^{eff} and D_p^{eff} can be computed [12–15] from the velocity field $w(x,y)$ and the so called b-field $b(x,y)$.

$$W_p^{\text{eff}} = \frac{\int_{\Omega_p} w(x,y)\mathrm{d}x\mathrm{d}y}{\int_{\Omega_p} \mathrm{d}x\mathrm{d}y}, \quad \begin{aligned} D_p^{\text{eff}} &= D_p + D_p \frac{\int_{\Omega_p} ||\nabla_\perp b||^2}{\int_{\Omega_p} \mathrm{d}x\mathrm{d}y} \\ &= D_p + \frac{\int_{\Omega_p} b\left(W_p^{\text{eff}} - w\right)\mathrm{d}x\mathrm{d}y}{\int_{\Omega_p} \mathrm{d}x\mathrm{d}y} \end{aligned} \tag{4}$$

where $\nabla_\perp = \partial/\partial x \mathbf{e}_x + \partial/\partial x \mathbf{e}_y$ is the cross-sectional gradient-operator and the b-field is obtained from the solution of a 2D steady-state elliptical equation equipped with Neumann boundary condition on the boundary $\partial\Omega_p$ of the effective particle domain Ω_p:

$$D_p \nabla_\perp^2 b(x,y) = W_p^{\text{eff}} - w(x,y) \tag{5}$$

Relying on the effective transport parameters W_p^{eff} and D_p^{eff}, governing the dynamics of the particle swarm after a transient time necessary for the particles to explore the entire cross section, it is possible to evaluate the minimum column $L_{\min}$ ensuring an accurate peak separation. Let M_{ij} be the minimum length to obtain a unitary resolution R_{ij} between pairs of particles (i,j), i.e., a 2.3 % overlap between the (supposedly Gaussian) chromatograms of i and j particle swarms at the outlet section. Indeed, the peak resolution $R_{ij}(L)$ that is attained at a device length L (downstream) can be estimated from the average residence times $<t_i>$ and $<t_j>$ and the squared variances σ_i^2 and σ_j^2 of the Gaussian distributions of particles i and j:

$$R_{ij}(L) = \frac{\langle t_i \rangle - \langle t_j \rangle}{2\left(\sigma_i + \sigma_j\right)}, \quad < t_i \ge \frac{L}{W_i^{\text{eff}}}, \quad \sigma_i^2 = \frac{2\,L\,D_i^{\text{eff}}}{\left(W_i^{\text{eff}}\right)^3} \tag{6}$$

Therefore, the minimum column length M_{ij} to obtain a unitary resolution between i and j particles can be estimated as:

$$R_{ij}\left(M_{ij}\right) = 1 \Rightarrow M_{ij} = 8 \left(\frac{\sqrt{\dfrac{D_i^{\text{eff}}}{\left(W_i^{\text{eff}}\right)^3}} + \sqrt{\dfrac{D_j^{\text{eff}}}{\left(W_j^{\text{eff}}\right)^3}}}{\dfrac{1}{W_i^{\text{eff}}} - \dfrac{1}{W_j^{\text{eff}}}} \right)^2 \tag{7}$$

For a three-particle mixture, three resolutions can be defined, namely, R_{12} (large-medium particles), R_{23} (medium-small particles), and R_{13} (large-small particles) and correspondingly three minimum lengths M_{12}, M_{23}, and M_{13}. Therefore, the minimum length $L_{\min}$ ensuring the required resolution of the three peaks is:

$$L_{\min} = \max(M_{12}, M_{23}, M_{13}) \tag{8}$$

This estimate of the minimum length $L_{\min}$ based on Eqs. (7) and (8) is valid when the macrotransport regime has been reached. In the standard HDC separation, the column length necessary to achieve the asymptotic regime is negligible compared to the total length, because all the particles, small, medium, and large, are uniformly distributed at the inlet section. On the contrary, in the (DBS)-HDC, a transient length $L_T(d_p)$ for medium and small particles must be estimated and accounted for a safe estimate of the minimum length to get a complete resolution between the three-size of particles. Indeed, since all the particles are injected in the core channel, it is necessary to consider the length downstream that small and medium particles need to travel before exploring the whole section to which they have access through the slit openings.

This initial column segment length $L_T(d_p)$ necessary for medium ($d_p = d_2$) and small particles ($d_p = d_3$) to reach a uniform distribution on the accessible cross-sectional domain Ω_p can be estimated as [13, 14]:

$$L_T\left(d_p\right) \simeq H \frac{Pe_p}{\nu_p}, \quad Pe_p = \frac{UH}{D_p} \tag{9}$$

where Pe_p is the particle Péclet number, U is the mean eluent velocity, H is a characteristic length here taken equal to the edge of the internal core channel, and ν_p is the dominant eigenvalue of the cross-sectional diffusion operator $\nabla_\perp^2$ acting on the cross-sectional domain Ω_p accessible to medium-sized and smaller particles and equipped with Neumann boundary condition on $\partial\Omega_p$.

Therefore, a safe estimate of the minimum length $L_{\min}$ for the DBS-HDC device, accounting for the transient lengths $L_T(d_1)$ and $L_T(d_2)$ of medium and small particles, reads as follows:

$$L_{\min}^{\text{DBS-HDC}} = \max(N_{12}, N_{23}, N_{13}) \tag{10}$$

$$N_{12} = M_{12} + L_T(d_2), \quad N_{23} = M_{23} + \max(L_T(d_2), L_T(d_3)),$$
$$N_{13} = M_{13} + L_T(d_3) \tag{11}$$

Research Article

where N_{12}, N_{23}, and N_{13} are the actual lengths to obtain a complete peak separation between large-medium particles (1,2), medium-small particles (2,3), and large-small particle (1,3).
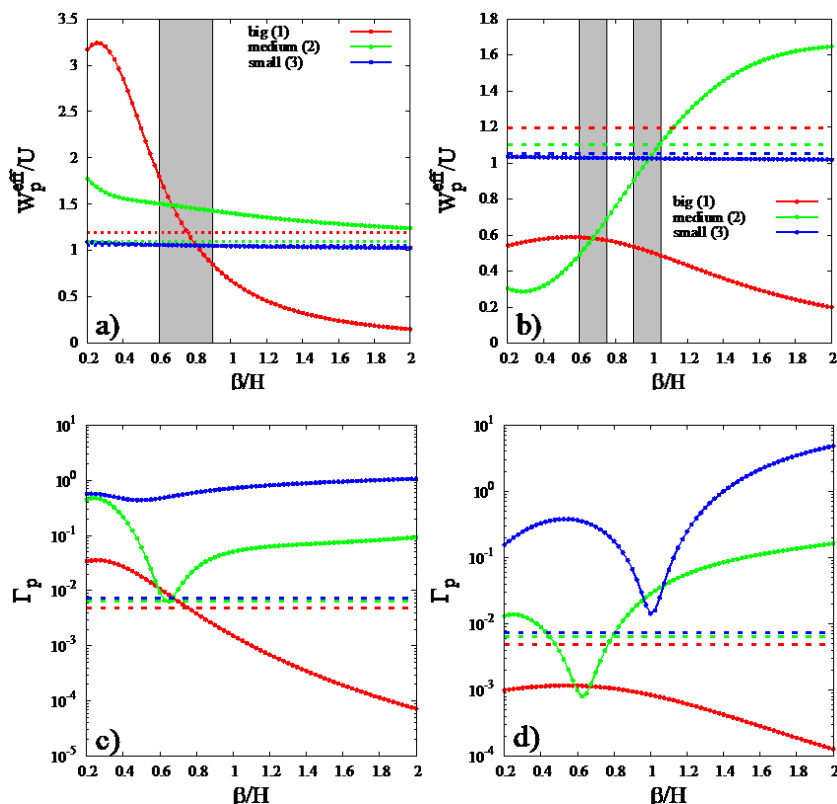
3 Results and Discussion

The effective parameters and the separation performance of the DBS-HDC device are investigated for almost 200 different geometries, characterized by different widths of the external (γ) and of the intermediate (β) coaxial channels, keeping fixed the core channel area (side length H). The final goal is to find the best configuration to separate a three-particle mixture and to compare the performance of the optimized geometry with that of an HDC column operating under the same conditions (same side length H and same eluent flow velocity).

3.1 Effective Transport Parameters

The DBS mechanism allows to modulate the eluent velocity field in the three channels by changing the two thicknesses γ and β. Three different axial velocity profiles are shown in Fig. 3 to highlight how, by varying γ and β, it is possible to localize the maximum intensity of the axial velocity at different positions of the cross-sectional domain Ω.

Different axial velocity profiles imply various effective velocities of the three sets of particles. Figs. 4a and 4b demonstrate the behavior of the normalized effective velocity W_p^{eff}/U of small, medium, and large particles as a function of β/H for a small and a large value of γ, namely, $\gamma/H = 0.25$ and $\gamma/H = 1$, thus highlighting how it is possible to obtain large differences between the effective velocities of the different particles, much larger (one order of magnitude) than those attained in HDC.

It can be further observed that, by changing the thickness β of the intermediate channel it is possible to change the temporal order according to which different particles are eluted. Indeed, for $\gamma/H = 0.25$ (Fig. 4a), large particles are eluted first for $\beta/H < 0.5$

because $W_1^{\text{eff}} > W_2^{\text{eff}} > W_3^{\text{eff}}$ while $W_2^{\text{eff}} > W_3^{\text{eff}} > W_1^{\text{eff}}$ (medium particles are eluted first and large particles are eluted last) for $\beta/H > 1$. The scenario changes completely for $\gamma/H = 1$ (Fig. 4b) where, for $\beta/H < 0.5$, small particles are faster than medium and small ones. Grey regions indicate values of β/H that should be avoided because different particles have the same velocity and cannot be separated (minimum length goes to infinity).

The drawback of the DBS mechanism is that it amplifies the axial dispersion especially of medium and small particles as shown in Figs. 4c and 4d in terms of the Taylor-Aris dispersion coefficient γ_p, relating the normalized effective dispersion coefficient D_p^{eff}/D_p to the particle Péclet number Pe_p:

$$D_p^{\text{eff}}/D_p = 1 + \Gamma_p Pe_p^2 \tag{12}$$
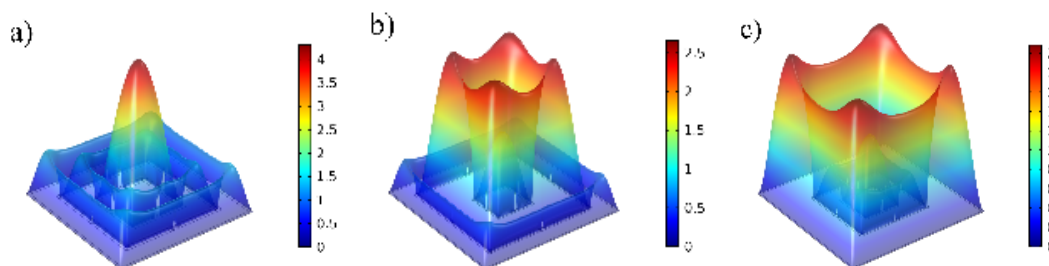

Figure 4. Normalized effective particle velocity W_p^{eff}/U and Taylor-Aris dispersion coefficient γ_p vs. β/H for $\gamma/H = 0.25$ (a, c) and $\gamma/H = 1$ (b, d). Dashed lines indicate the same quantities for the standard HDC. Grey regions indicate the no-separation range.


Figure 3. Normalized axial velocity profile $w(x,y)/U$ of the eluent for three different geometries of the DBS-HDC device. (a) $\beta/H = 0.5$, $\gamma/H = 0.5$; (b) $\beta/H = 1$, $\gamma/H = 0.5$; (c) $\beta/H = 0.5$, $\gamma/H = 1$.

However, as will be shown below, if the DBS-HDC channel is properly designed, the effect of the increased axial dispersion is overshadowed by the higher difference between particles effective velocities.

3.2 Separation Efficiency

According to Eq. (7), from W_p^{eff} and D_p^{eff} with $p = 1, 2, 3$, is possible to estimate the three minimum lengths M_{12}, M_{23}, and M_{13} for any set of geometric parameters (β,γ). A further step is required to estimate the dominant eigenvalue ν_p of $\nabla_\perp^2$ controlling the transient length $L_T(d_p)$ for medium $(d_p = d_2)$ and small particles $(d_p = d_3)$.

Fig. 5 shows the behavior of ν_p vs. β/H for $d_p = d_2, d_3$ and three increasing values of γ. The smaller ν_p, the larger the transient length, Eq. (9). The eigenvalue ν_2 of medium particles is a decreasing function of β and unaffected by the thickness γ of the external channel because $\text{meas}(\Omega_p) \simeq (1 + 2\beta)^2$ for $d_p = d_2$. The eigenvalue ν_3 of small particles decreases with β and γ because $\text{meas}(\Omega_p) \simeq (1 + 2\gamma + 2\beta)^2$ for $d_p = d_3$.
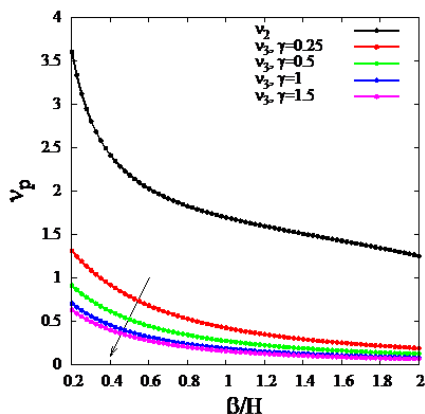
Figure 5. Dominant eigenvalue ν_p vs. β/H for $d_p = d_2$ (ν_2, medium particles) and $d_p = d_3$ (ν_3, small particles) for $\gamma/H = 0.25, 0.5, 1, 1.5$.

From M_{12}, M_{23}, M_{13}, $L_T(d_2)$, and $L_T(d_3)$, the three minimum lengths N_{12}, N_{23}, N_{13} and therefore the minimum device length $L_{\min}(\beta,\gamma,Pe)$ can be estimated ensuring the required peak resolution according to Eqs. (10) and (11).

Figs. 6a and 6b show the behavior of N_{12}, N_{23}, N_{13} and $L_{\min}$ (green curve) as a function of β for a small and a large value of γ, namely, $\gamma/H = 0.25$ and $\gamma/H = 1$. The figure refers to an eluent velocity U corresponding to a Péclet number[2] $Pe = Pe_1 = 10^3$
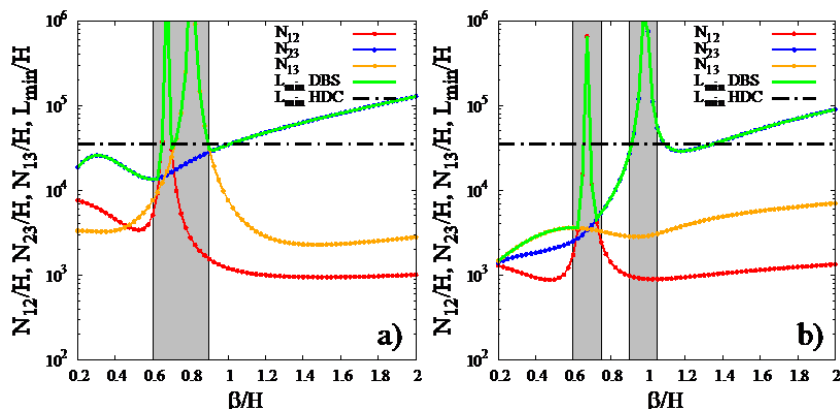
Figure 6. Minimum lengths N_{12}, N_{23}, N_{13} and $L_{\min}$ vs. β/H for $\gamma/H = 0.25$ (a) and $\gamma/H = 1$ (b) at $Pe = Pe_1 = 10^3$. Dot-dash line represents $L_{\min}$ for standard HDC. Grey regions indicate the no-separation range.

representative of typical operating conditions[3]. The dot-dash line in Figs. 6a and 6b is the minimum length for a standard HDC column operating at the same Pe value. It can be readily observed that, for $0.2 < \beta < 0.6$ and $\gamma/H = 1$, the DBS-HDC device is about 20 times smaller than the standard HDC column.

Even better results can be obtained by further increasing the γ thickness as indicated in Fig. 7a where the ratio $L_{\min}^{\text{HDC}}/L_{\min}^{\text{DBS−HDC}}$ is plotted as a function of β/H for $\gamma/H = 1.5$ and $Pe = 100, 200, 1000$. It can be observed that for $\beta/H \approx 0.2$, the minimum length $L_{\min}^{\text{DBS−HDC}}$ is more than 30^times smaller than $L_{\min}^{\text{HDC}}$ in the whole range of Pe values investigated.

The optimal geometry with a small $\beta/H \approx 0.2$ and a large $\gamma/H \approx 1.5$ must be preferred not only because it corresponds to a much smaller device length $L_{\min}$ but also because it requires shorter times to perform a chromatographic experiment. The time interval $t_{\min}$ required to complete the separation is controlled by the elution time $\langle t_s \rangle$ and the half band-width $2\sigma_s$ of the slower particle swarm, identified with the subscript "s":

$$t_{\min} = \langle t_s \rangle + 2\sigma_s = \frac{L_{\min}}{W_s^{\text{eff}}} + \sqrt{\frac{L_{\min}D_s^{\text{eff}}}{\left(W_s^{\text{eff}}\right)^3}} \qquad (13)$$

For a standard HDC, the slower particle is always the smaller one, i.e., $s = 3$, while for the DBS-HDC device it depends on the geometric parameters (β,γ). For the optimal geometric configuration identified $(\beta/H,\gamma/H) = (0.2,1.5)$ the slower particle swarm is the medium-sized one, i.e., $s = 2$. Numerical results for the ratio $t_{\min}^{\text{HDC}}/t_{\min}^{\text{DBS−HDC}}$ as a function of β/H are depicted in Fig. 7b for $\gamma/H = 1.5$ and $Pe = 100, 200, 1000$ (same operating conditions considered in Fig. 7a). The DBS-HDC device is about three times faster than HDC for $0.2 < \beta/H < 0.6$ in the whole range of Pe values investigated.

---

2) The particle Péclet number Pe_1, associated with the larger particles, is taken as representative of the operating conditions and simply denoted as Pe. Because all the particles are entrained in the same flow (i.e., associated with the same average velocity U of the eluent), on the assumption that the diffusion coefficient can be estimated from the Stokes-Einstein relationship, it is obtained that $Pe_2 = (d_2/d_1)Pe_1$ and $Pe_3 = (d_3/d_1)Pe_1$.

3) By setting the core channel side length H 10 times larger than the large particle diameter $H = 10d_1$, the reference Péclet number can be estimated at 298.15 K in water solution, as $Pe \cong 20.2\,U\,(d_1)^2$ with U expressed in $\mu m\,s^{-1}$ and d_1 in μm. Therefore, for a large particle with diameter d_1 in the range $[0.5\,\mu m : 2.0\,\mu m]$, the Pe value varies in the range $[500:8100]$ for an eluent average velocity $U = 100\,\mu m\,s^{-1}$.
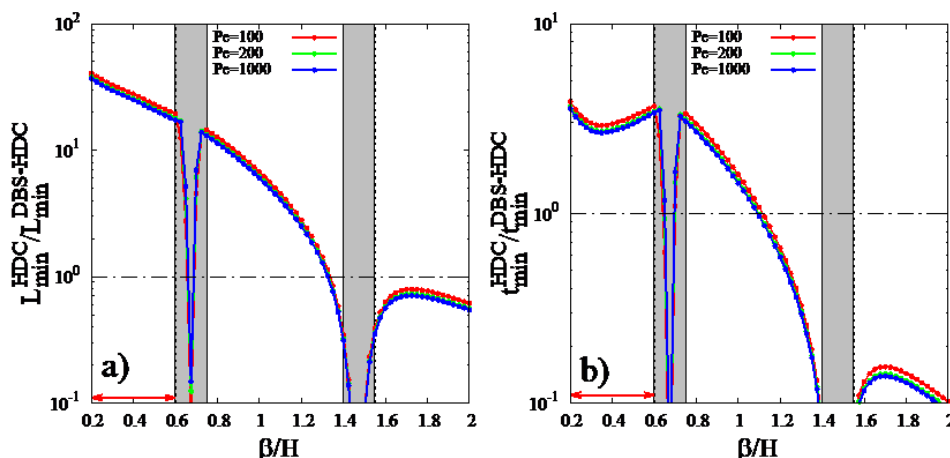
Figure 7. Minimum length ratio $L_{min}^{HDC}/L_{min}^{DBS-HDC}$ and minimum time ratio $t_{min}^{HDC}/t_{min}^{DBS-HDC}$ vs. β/H for $\gamma/H = 1.5$ and $Pe = 100, 200, 1000$. Grey regions indicate the no-separation range.

4 Conclusions

The miniaturization of HDC-based analyses, allowed by micro-fabrication technique and 3D printing techniques, opens unprecedented possibilities for new design concepts. The Brownian sieving device analyzed in this article constitutes a recent example of a new class of highly performing microfluidic devices characterized by simple channel geometries that do not require the presence of a disordered stationary phase. The chosen geometry, ideally suited for 3D nanoprinting, stretches to the boundary of the current resolution for this technology. If the separation of micrometer-sized analytes is sought, current 3D-nanoprinting techniques should be sufficiently accurate to the scope.

In this work, the enforcement of a double Brownian sieving mechanism has been considered for a three-particle suspension. Optimal geometric parameters have been identified based on the macrotransport approach (moment analysis), which allows a computationally convenient framework to predict the device performance. The results are extremely encouraging as they show up to 3000 % improvement over standard micro-capillary HDC.

Acknowledgment

The authors have declared no conflict of interest.

Symbols used

$b(x,y)$	[–]	b-field
$C(z,t)$	[mol/m³]	cross-section average concentration
d_1, d_2, d_3, d_p	[m]	particle diameters
D_p	[m²/s]	particle diffusivity
D_p^{eff}	[–]	effective dispersion coefficient

H	[m]	core channel side length (reference length)
L_{min}	[m]	minimum device length
$L_T(d_p)$	[m]	transient length of particle with diameter d_p
$n(x,y,z,t)$	[–]	particle number density
N_{ij}	[m]	minimum length to obtain a complete peak separation between pairs of particles i and j
p	[Pa]	hydrodynamic pressure
Pe_p	[–]	particle Péclet number
R_{ij}	[–]	resolution between pairs of particles i and j
$<t_i>$	[s]	average residence time of particle i
t_{min}	[s]	minimum time of the experiment
U	[m/s]	average eluent velocity
$w(x,y)$	[m/s]	axial velocity profile
W_p^{eff}	[–]	effective velocity
x, y, z	[–]	spatial coordinates

Greek letters

β	[–]	thicknesses of the intermediate annular channel
γ	[–]	thicknesses of the external annular channel
γ_p	[–]	Taylor-Aris dispersion coefficient
λ_1, λ_2	[m]	width of the slit openings
μ	[Pa s]	fluid viscosity
ν_p	[–]	dominant eigenvalue of the cross-sectional Laplace operator $\nabla_\perp^2$
σ_i^2	[m²]	variance of the Gaussian distributions of particle i

Abbreviations

DBS	double Brownian sieving
HDC	hydrodynamic chromatography

References

[1] L. Pitkänen, A. R. Montoro Bustos, K. E. Murphy, M. R. Winchester, A. M. Striegel, *J. Chromatogr. A* **2017**, *1511*, 59–67. DOI: https://doi.org/10.1016/j.chroma.2017.06.064

[2] Y. Fan, M. Marioli, K. Zhang, *J. Pharm. Biomed. Anal.* **2021**, *192*, 113642. DOI: https://doi.org/10.1016/j.jpba.2020.113642

[3] L. Calzolai, D. Gilliland, C. Pascual Garcìa, F. Rossi, *J. Chromatogr. A* **2011**, *1218 (27)*, 4234–4239. DOI: https://doi.org/10.1016/j.chroma.2011.01.017

[4] C. Contado, *Anal. Bioanal. Chem.* **2017**, *409*, 2501–2518. DOI: https://doi.org/10.1007/s00216-017-0180-6

[5] E. Chmela, R. Tijssen, M. T. Blom, H. J. G. E. Gardeniers, A. van den Berg, *Anal. Chem.* **2002**, *74 (14)*, 3470–3475. DOI: https://doi.org/10.1021/ac0256078

[6] A. M. Striegel, A. K. Brewer, *Annu. Rev. Anal. Chem.* **2012**, *5*, 15–34. DOI: https://doi.org/10.1146/annurev-anchem-062011-143107

[7] A. M. Striegel, *Anal. Bioanal. Chem.* **2012**, *402*, 77–81. DOI: https://doi.org/10.1007/s00216-011-5334-3

[8] S. H. Holm, J. P. Beech, M. P. Barrett, J. O. Tegenfeldt, *Lab Chip* **2011**, *11 (7)*, 1326–1332. DOI: https://doi.org/10.1039/C0LC00560F

[9] A. Adrover, S. Cerbelli, *Phys. Fluids* **2017**, *29*, 062005. DOI: https://doi.org/10.1063/1.4986827

[10] A. Adrover, S. Cerbelli, M. Giona, *Phys. Fluids* **2018**, *30*, 042002. DOI: https://doi.org/10.1063/1.5022257

[11] M. Murmura, A. Adrover, S. Cerbelli, *Eur. Phys. J.: Spec. Top.* **2019**, *228 (1)*, 5–23. DOI: https://doi.org/10.1140/epjst/e2019-800142-1

[12] V. Biagioni, A. Adrover, S. Cerbelli, *Processes* **2019**, *7 (8)*, 498. DOI: https://doi.org/10.3390/pr7080498

[13] V. Biagioni, G. Balestrieri, A. Adrover, S. Cerbelli, *Biosensors* **2020**, *10 (9)*, 126. DOI: https://doi.org/10.3390/bios10090126

[14] V. Biagioni, A. Sow, A. Adrover, S. Cerbelli, *Anal. Chem.* **2021**, *93 (17)*, 6808–6816. DOI: https://doi.org/10.1021/acs.analchem.1c00780

[15] V. Biagioni, A. Sow, A. G. Fagiolo, A. Adrover, S. Cerbelli, *J. Chromatogr. A* **2021**, *1659*, 462652. DOI: https://doi.org/10.1016/j.chroma.2021.462652

[16] C. Venditti, S. Cerbelli, G. Procopio, A. Adrover, *Phys. Fluids* **2022**, *34*, 042010. DOI: https://doi.org/10.1063/5.0088977

[17] *Macrotransport Processes* (Eds: H. Brenner, D. A. Edwards), Elsevier, New York **1993**.

Research Article: An innovative separation microdevice based on a Brownian sieving effect coupled with hydrodynamic chromatography is proposed to investigate and optimize a modified geometry suitable for obtaining the simultaneous separation of a three-size diluted suspension. The results prove a significant improvement of up to 3000 % over the standard hydrodynamic chromatography.

Fractionation of a Three-Particle Mixture by Brownian Sieving Hydrodynamic Chromatography

Valentina Biagioni, Claudia Venditti, Alessandra Adrover*, Stefano Cerbelli